Jurnal Teknologi

Full paper

Soot Particle Evolution and Transport in a Direct Injection Diesel Engine

Muhammad Ahmar Zuber, Wan Mohd Faizal Wan Mahmood*, Zambri Harun, Zulkhairi Zainol Abidin

Department of Mechanical and Materials Engineering, Faculty of Engineering and Built Environment, Universiti Kebangsaan Malaysia, 43600 Bangi, Selangor, Malaysia

*Corresponding authors: faizal.mahmood@ukm.edu.my

Article history

Received : 7 January 2015
Received in revised form :
7 March 2015
Accepted : 8 April 2015

Graphical abstract

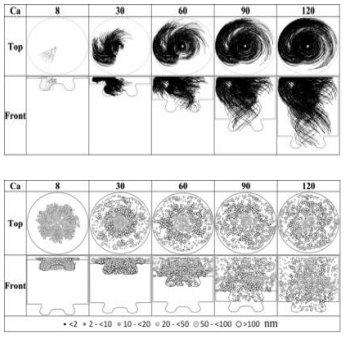

Abstract

Particle-based in-cylinder soot distribution study is becoming more important as the rules and regulations pertaining to particulate emission of diesel-powered vehicles have been increasingly more stringent. This paper focuses on the investigation of soot size evolution and its distribution and transport inside an engine cylinder. The overall process of soot formation includes soot nucleation, surface growth, oxidation, coagulation and agglomeration. The present study considers only soot surface growth, oxidation and coagulation to predict the in-cylinder soot particle size. The soot surface growth model was based on Hiroyasu's soot formation model while soot oxidation was referred to Nagle & Strickland-Constable's soot oxidation model. Coagulation rate was defined using Smoluchowski's equation with constant proposed by Wersborg. From this study, it is demonstrated that soot particles with relatively larger size are gathered in the centre of the cylinder while smaller soot particles are found to be in the region near the wall. Soot number density is considerably high at the start of combustion and reduces sharply afterward while the soot particle size shows the opposite trend. Soot formation rate was found to be dominant at earlier crank angle and is overcome by soot oxidation and coagulation processes that caused lower soot number density but higher soot particle size.

Keywords: Particle tracking; in-cylinder soot; coagulation; diesel engine

Abstrak

Kajian taburan partikel jelaga di dalam enjin diesel telah menjadi semakin penting kerana undang-undang dan peraturan yang dikenakan terhadap pelepasan bahan cemar oleh kenderaan berenjin diesel semakin diperketatkan. Kajian ini memfokuskan kepada evolusi saiz partikel jelaga serta taburann dan pergerakan partikel jelaga di dalam silinder enjin diesel. Proses pembentukan jelaga adalah merangkumi proses nukleasi, pertumbuhan permukaan, pengoksidaan, koagulasi dan aglomerasi. Tetapi dalam kajian ini hanya proses pertumbuhan permukaan, pengoksidaan dan koagulasi yang diambil kira bagi meramal saiz partikel jelaga di dalam silinder enjin. Model pertumbuhan permukaan jelaga adalah berdasarkan model pembentukan jelaga Hiroyasu manakala model pengoksidaan disandarkan kepada model pengoksidaan Nagle & Strickland-Constable. Kadar koagulasi dalam bentuk persamaan Smoluchowski menggunakan pekali yang telah dicadangkan oleh Wersborg. Hasil kajian ini menunjukkan partikel jelaga dengan saiz yang besar berkumpul ditengah silinder enjin manakala partikel jelaga yang lebih kecil dijumpai sekitar dinding silinder. Ketumpatan bilangan partikel jelaga yang tinggi pada permulaan pembakaran berkurang secara mendadak manakala saiz partikel jelaga menunjukkan trend yang sebaliknya. Kadar pembentukan jelaga adalah lebih dominan pada sudut engkol terawal tetapi selepas itu diatasi oleh kadar proses pengoksidaan dan koagulasi yang menyebabkan berlaku pengurangan pada ketumpatan bilangan jelaga tetapi peningkatan pada saiz partikel jelaga.

Kata kunci: Penjejakan patikel; jelaga dalam silinder; koagulasi; enjin diesel

1.0 INTRODUCTION

Soot is an unwanted by-product of combustion generated mostly by burning of fossil fuels. The formation of soot inside engine cylinders during the combustion is yet to be fully understood. The studies of soot become a centre in today's research because of the growing concerns towards pollution and strict regulations regarding soot emission. Various studies on in-cylinder soot modelling had been carried out to further understand the process of soot formation in an engine. A study by Appel *et al.* [1] reported a detailed kinetic model of soot formation using a combination of gas-phase reaction, aromatic chemistry, soot particle coagulation, soot particle aggregation and soot surface growth. However, the model still contains uncertainty of thermodynamic and kinematic

of aromatic and soot chemistry. While Frenklach[2] classified the formation of soot into four major process, namely homogeneous nucleation of soot particles, particle coagulation, particle surface reactions (growth and oxidation) and particle agglomeration. Mosbach *et al.*[3] proposed the soot formation in internal combustion not only limited to soot mass, number density, volume fraction and surface area but also included the soot morphology and chemical composition of soot aggregates.

In in-cylinder engine combustion, Frenklach[2] and Maricq[4] observed that soot initially has spherical shape and later requires fractal shape due to the coagulation. According to Frenklach[2] soot coagulation control the evolution of the soot particle number density and soot was modelled using either a discrete-sectional method or the method of moment. In his research, soot particle coagulation can be divided into two stages, coalescent growth and agglomeration into fractal growth. In coalescent growth, the soot particles collide with each other and form new particles. Then the soot particles start to agglomerate and form chain-like structure. During the agglomeration process, the transition from coalescent growth to fractal growth takes place but the fractal growth is not well understood.

Wersborg *et al.*[5] proposed a different mathematical model to evaluate soot particle coagulation. Using Smoluchowski's coagulation model with specific coagulation rate constant, *K*, coagulation rate was defined. Kazakov and Frenklach[6] used method of moment to determine the dynamic of soot coagulation while other researchers proposed different approaches which can be reviewed in.[4,7-10]

All of these studies, however, gave less emphasis to the history of movement and transport of in-cylinder soot particles. Besides soot particle size, this paper also discusses the history of soot particle movements. The soot pathline, soot particle size and size distribution in this paper was predicted by post-processing previous CFD data.

2.0 NUMERICAL METHOD

The simulation of in-cylinder combustion was performed by[11] using Kiva-3V release II CFD software to produce a mass-based in-cylinder soot distribution in previous study. The details of engine specifications, models used and computational setup can be found in the paper. A distribution of soot concentration (g/cm^3) from the CFD simulation within a selected range of crank angles is shown in Figure 1. This information became the essential information for subsequent particle-based soot distribution study reported in this paper.

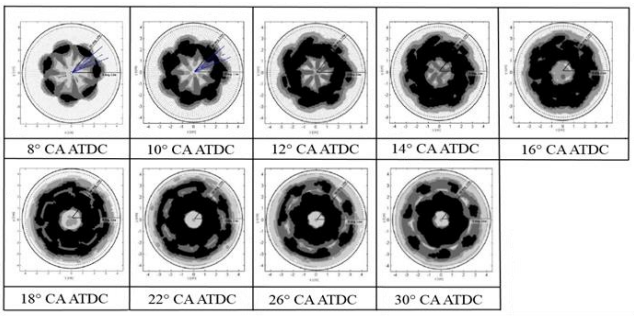

(> 0 g/cm^3, > 1×10^{-7} g/cm^3, > 1×10^{-6} g/cm^3, > 1×10^{-5} g/cm^3)

Figure 1 Soot concentration distribution within a selected range of crank angles showing clockwise bulk flow

The results from this simulation such as bulk gas velocity, temperature, pressure and concentration of gases and other species were obtained and post processed using series of Matlab routines to predict the pathline, soot particle size and size distribution inside the engine cylinder. The prediction was started at 8° and ended at 120° CA ATDC during the power stroke. Fourth order Runge-Kutta method and trilinear interpolation technique were included in the soot particle tracking routine to predict the position and pathline of each soot particle by applying Equation (1) where s_n is the current soot particle position, t_n the current time step and Δt the time-step duration.

$$s_{n+1} = s_n + u(s_n, t_n)\Delta t \tag{1}$$

To calculate soot particle numbers and size in the present study, chemical and physical processes of surface growth, oxidation, and coagulation were considered. Assumption was made that the soot movements inside the engine cylinder follow the velocity vector of bulk flow field and soot particles are massless. Soot particles were also assumed spherical with constant density of 2 g.cm^{-3} throughout the combustion process.

At each time step, Hiroyasu's soot formation model expressed in Equation (2) and Nagle & Strickland-Constable (NSC) soot oxidation model in Equation (3) were considered to calculate the soot mass change. In Equation (2) M_{sfi} represents the soot mass formed, M_{fvi} represents the soot concentration of fuel vapour, which is considered as the source of soot, P is the pressure, N is soot particle formation multiplication factor and T is temperature. E_{sf} which is equal to 12500 cal/mole, is the activation energy and R, 1.987 cal/mole-K, is the universal gas constant. In Equation (3), $\dot{R}_{NSC}$ represents the rate of carbon surface oxidation in g.cm^{-2}.s.

$$\frac{dM_{sfi}}{dt} = NM_{fvi}P_i^{0.5}e^{(E_{sf}/RT_i)} \tag{2}$$

$$\dot{R}_{NSC} = \left(\frac{k_A P}{1+k_z P}\right)x + k_B P(1-x) \tag{3}$$

x is defined as

$$x = \frac{1}{1+(k_T/k_B)p} \tag{4}$$

whereas k_A, k_B, k_T and k_Z values are as in Equation (5)-(8).

$$k_A = 20\times e^{-30{,}000/RT} \quad \text{g cm}^{-2}\,\text{s}^{-1}\,\text{atm}^{-1} \tag{5}$$

$$k_B = 4.46\times10^{-3}\times e^{-15{,}200/RT} \quad \text{g cm}^{-2}\,\text{s}^{-1}\,\text{atm}^{-1} \tag{6}$$

$$k_T = 1.51\times10^{5}\times e^{-97{,}00/RT} \quad \text{g cm}^{-2}\,\text{s}^{-1} \tag{7}$$

$$k_Z = 21.3\times e^{4{,}100/RT} \quad \text{atm}^{-1} \tag{8}$$

Coagulation model used in this paper was based on work in.[5] The coagulation rate was stated in the form of Smoluchowski as in Equation (9) where K is the coagulation rate constant as shown in Equation (10).

$$\dot{N}_c = \frac{1}{2} K n^2 \quad (9)$$

$$K = 16 a^2 y \left(\frac{\pi k T}{m} \right)^{1/2} \quad (10)$$

Correction for inter-particle forces denoted as y was set to 30 according to [5], a equal to 1.00×10^{-8} m, Boltzmann constant k value is 1.38×10^{-23} $m^2.kg/s^2.K^{-1}$, temperature T is 1600 K, and particle mass m, is 8.38×10^{-21} kg. K was calculated and considered constant with the value of 5×10^{-8}.

4.0 RESULTS AND DISCUSSION

Soot particle pathlines were generated using Matlab plotting and the results were presented in Figure 2. The pathlines shown in this figure were the representative pathlines for one seventh of the cylinder. The pathlines display a clock-wise direction following the swirl pattern set during the CFD simulation. It can also be observed that soot moved closer the cylinder wall as early as 30° CA ATDC and more soot particles moved to this region at later crank angles. At 120° CA ATDC, soot was found to be transported to most areas in the cylinder.

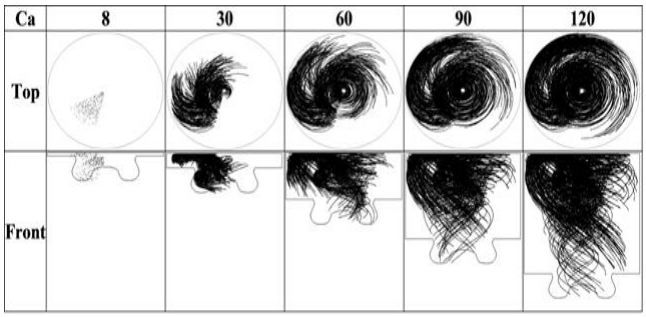

Figure 2 Soot particle pathlines inside an engine cylinder starting from 8 CA ATDC and ending at 120 CA ATDC

Besides soot pathlines, it is also important to know its particle size at different locations in the cylinder in order to predict further transport of the soot particles. Graphical distribution of soot particle size with different size range is shown in Figure 3. It presents the in-cylinder size distribution at selected crank angles and shows that the soot particles with relatively larger size formed at the core of fuel spray and tend to accumulate at the centre of the cylinder while soot particles that moved near the cylinder wall boundary were smaller which is most likely due to higher oxidation rate which agrees well with.[12] The range of soot particle size in the squish region near the cylinder wall is between 10 to 50 nm.

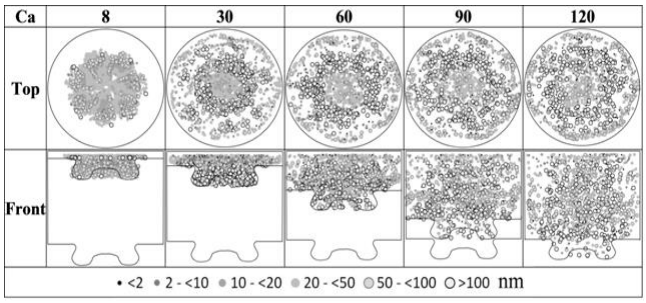

Figure 3 In-cylinder soot particle distribution

Soot number density and size distribution can be observed in Figure 4. As shown in the figure, the average soot particle size starts at 30 nm and the average particle size increases up to 80 nm at 120° CA ATDC, whereas, soot particle number density decreases to 5×10^{13} at 120° CA ATDC from 2×10^{14} at 8° CA ATDC. Significant soot particle size increase and particle number density reduction is mainly caused by the process of coagulation of soot particles overshadowing the other processes namely surface growth and oxidation. The soot size distribution can be observed in Figure 5 where at 8° CA ATDC the distribution is in Gaussian distribution peaks at size range of 20-50 nm. Later as the combustion continues to higher crank angles, the graph shows a bimodal lognormal distribution to larger size of 50-100 nm and bigger than 100 nm due to the coagulation process.[3,6] also found that at later crank angles the size distribution turned bimodal.

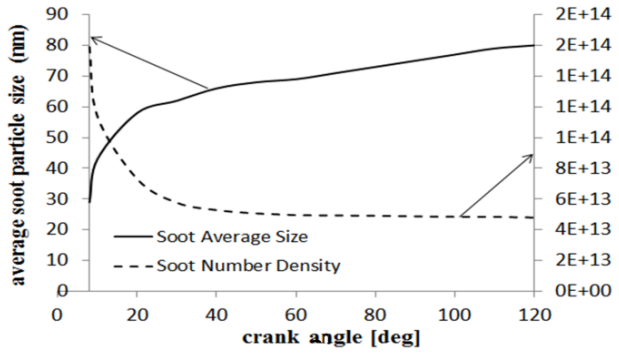

Figure 4 Average soot particle size (nm) and soot particle number density (number of particles/cm^3)

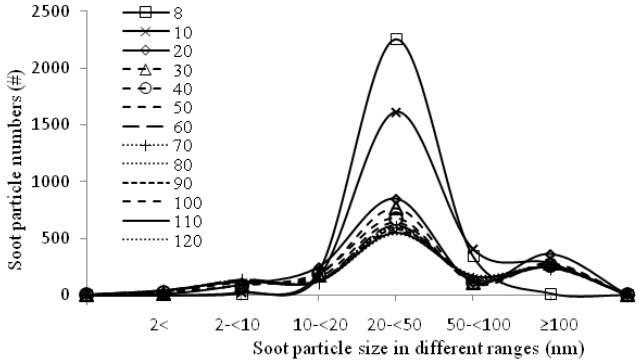

Figure 5 Distribution of soot of different sizes at different crank angles

Figure 6 shows a decreasing trend of both in-cylinder temperature and pressure with crank angles. The pressure profile was similar with work done by Mosbach *et al*. and Menkiel.[3,12] In Figure 7, it shows that at earlier combustion, combination of surface growth and coagulation rates were higher than the oxidation rate, but gradually flatten and finally match at later crank angles. As early as 15° CA ATDC, oxidation starts to dominate as surface growth rate rapidly decreases. As a results, in combination of coagulation process, soot size increases exponentially and soot number density starts to reduce as shown previously in Figure 4.[13-15] These results agree with statement by Appel *et al*.[1] which says that at higher temperature soot particle become more reactive and tendency to oxidize higher as compared to lower temperature soot particle.

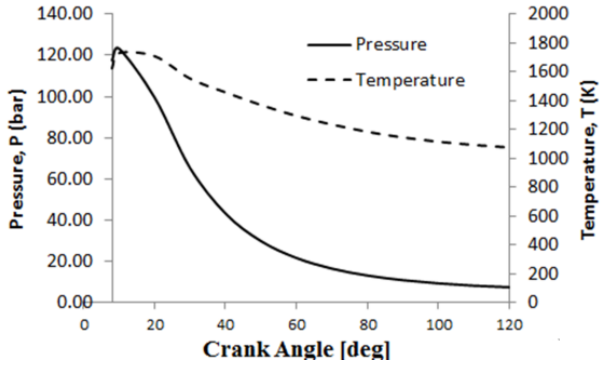

Figure 6 Average in-cylinder pressure and temperature

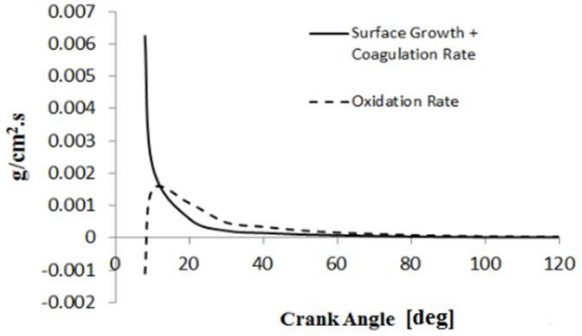

Figure 7 Soot growth and oxidation rates

■4.0 CONCLUSIONS

The soot formation processes considered in the present study were surface growth, oxidation and coagulation processes as an extension of the previous work.[16] Average soot particle size starts at 20 nm and increases throughout the combustion due to the coagulation process. During the progress of combustion, temperature, pressure, soot number density and oxidation rate decrease until the end of simulation recorded. On the other hand, surface growth rate is high initially then decreases rapidly after 10° CA ATDC. Soot particle that are less than 50 nm in diameter tend to be transported to the region near the wall boundary and larger soot particles accumulate at the centre of the cylinder. Soot coagulation process significantly affects the soot particle size and soot number density throughout the combustion process.

Acknowledgements

This research was supported by Ministry of Education of Malaysia and Universiti Kebangsaan Malaysia under FRGS/1/2013/TK01/UKM/02/2 and GGPM-2011-055 research grants. Their financial supports are gratefully acknowledged.

References

[1] Appel J., Bockhorn H., and Frenklach M. 2000. Kinetic Modeling of Soot Formation with Detailed Chemistry and Physics: Laminar Premixed Flames of C_2 Hydrocarbons. *Combustion and Flame*. 121(1-2): 122–136.
[2] Frenklach M. 2002. Reaction Mechanism of Soot Formation in Flames. *Physical Chemistry Chemical Physics*. 4(11): 2028–2037.
[3] Mosbach S., Celnik M. S., Raj A., Kraft M., Zhang H. R., Kubo S., and Kim K. O. 2009. Towards A Detailed Soot Model for Internal Combustion Engines. *Combustion and Flame*. 156(6): 1156–1165.
[4] Maricq M. M. 2007. Coagulation Dynamics of Fractal-Like Soot Aggregates. *Journal of Aerosol Science*. 38(2): 141–156.
[5] Wersborg B. L., Howard J. B., and Williams G. C. 1973. Physical Mechanisms in Carbon Formation in Flames. *Symposium (International) on Combustion*. 14(1): 929–940.
[6] Kazakov A., and Frenklach M. 1998. Dynamic Modeling of Soot Particle Coagulation and Aggregation: Implementation With the Method of Moments and Application to High-Pressure Laminar Premixed Flames. *Combustion and Flame*. 114(3-4): 484–501.
[7] Graham S. C., Homer J. B., and Rosenfeld J. L. J. 1975. The Formation and Coagulation of Soot Aerosols Generated by the Pyrolysis of Aromatic Hydrocarbons. *Proceedings of the Royal Society A: Mathematical, Physical and Engineering Sciences*. 344(1637): 259–285.
[8] Kim D., Gautam M., and Gera D. 2002. Parametric Studies on the Formation of Diesel Particulate Matter Via Nucleation and Coagulation Modes. *Journal of Aerosol Science*. 33(12): 1609–1621.
[9] Sorensen C. M., Hageman W. B., Rush T. J., Huang H., and Oh C. 1998. Aerogelation in a Flame Soot Aerosol. *Journal of Aerosol Science*. 29: 623–624.
[10] Khan I. M., Wang C. H. T., and Langridge B. E. 1971. Coagulation and Combustion of Soot Particles in Diesel Engines. *Combustion and Flame*. 17(3): 409–419.
[11] Wan Mahmood W. M. F., Larocca A., Shayler P. J., Pegg I., and Bonatesta F. 2012. Predicted Paths of Soot Particles in the Cylinders of a Direct Injection Diesel Engine. *SAE International*. 2012-01-0148.
[12] Menkiel B. 2012. *Investigation of soot processes in an optical diesel engine*. Brunel University, United Kingdom.
[13] Cheng X., Chen L., Yan F., and Dong S. 2013. Study on Soot Formation Characteristics in The Diesel Combustion Process Based on an Improved Detailed Soot Model. *Energy Conversion and Management*. 75: 1–10.
[14] Puduppakkam K., Modak A., and Naik C. 2013. Soot Particle Tracking with FORTÉ CFD Using Method of Moments and a Detailed Soot Chemistry Mechanism. *International Multidimensional Engine Modeling User's Group Meeting*.
[15] Rao V., and Honnery D. 2014. Application of a Multi-Step Soot Model in a Thermodynamic Diesel Engine Model. *Fuel*. 135: 269–278.
[16] Zuber, M.A., Wan Mahmood W. M. F., Harun, Z., Zainol Abidin, Z., Larocca A., Shayler P. J., and Bonatesta F. 2015. Modeling of In-Cylinder Soot Particle Size Evolution and Distribution in a Direct Injection Diesel Engine. *SAE International*. 2015-01-1075.